Removal of Copper from Silicon Surfaces Using Hexafluoroacetylacetone (hfacH) Dissolved in Supercritical Carbon Dioxide

Bo Xie, Casey C. Finstad, and Anthony J. Muscat*

Department of Chemical & Environmental Engineering, University of Arizona, Tucson, Arizona 85721

Received July 5, 2002. Revised Manuscript Received October 28, 2004

Copper was etched from a silicon surface using the chelator hexafluoroacetylacetone (hfacH) dissolved in supercritical carbon dioxide ($scCO_2$) at 40−60 °C and 100−250 atm. Copper was deposited on Si(100) using doped HF solutions in the form of 10−90 nm Cu islands, as shown by scanning electron microscopy (SEM). X-ray photoelectron spectroscopy (XPS) indicated the islands were composed of $Cu(I)_2O$ due to air exposure before etching was attempted. Oxidation of the Cu(I) was performed using aqueous 30% H_2O_2 or a UV−Cl_2 gas phase, forming shells of Cu(II)O or $Cu(II)Cl_2$, respectively, surrounding cores of $Cu(I)_2O$. SEM images showed that the Cu(II)O had a flake morphology. The Cu(II) shells were removed selectively to the $Cu(I)_2O$ cores by processing with pure $scCO_2$ and rapidly releasing the system pressure (300 atm/min). Mechanical failure of the Cu(II)O and $Cu(II)Cl_2$ when CO_2 in stress corrosion cracks quickly expanded delaminated these layers, leaving only $Cu(I)_2O$ on the surface. Etching of both Cu(II) and Cu(I) was achieved when oxidized samples were processed in $scCO_2$ containing approximately 120 ppm of hfacH for 2 min. Nucleophilic attack of Cu(II) centers by hfacH formed copper(bis-hexafluoroacetylacetonate), $Cu(hfac)_2$ and water, or the monohydrate $Cu(hfac)_2{\cdot}H_2O$, which was soluble in $scCO_2$. The $Cu(hfac)_2{\cdot}H_2O$ byproduct is proposed to oxidize $Cu(I)_2O$ to Cu(II), allowing attack and etching by hfacH.

Introduction

Copper has replaced aluminum for interconnects in leading edge microelectronic devices to satisfy the demand for better performance. The lower resistivity of Cu ($\rho \sim 1.67$ $\mu\Omega$-cm) compared to Al ($\rho \sim 2.65$ $\mu\Omega$-cm) reduces the *RC* (*resistance* × *capacitance*) time constant, which improves the speed of signal transmission in a device.[1] Moreover, the larger mass of Cu than Al atoms significantly increases the electromigration lifetime of Cu interconnect wires.[2] The processing of Cu for device fabrication, however, is much more challenging than the deposition and etching technologies used for Al. The precursors for chemical vapor deposition (CVD) of Cu have relatively low volatilities, require high temperatures for uniform growth, and produce low growth rates. The primary obstacle to anisotropic etching of Cu for patterning is the low volatility of copper halides, which results in low etching rates. Instead of using CVD and plasma etching, Cu interconnect wires are fabricated using a dual damascene process, which involves physical vapor deposition of a Cu seed layer into the trenches in a dielectric film followed by electrolytic or electroless plating of a blanket Cu film and chemical mechanical planarization (CMP) to polish back down to the flat dielectric surface. The trenches of the dielectric must be covered with a barrier layer to prevent Cu from diffusing through the dielectric. Cleaning of the dielectric film before the barrier is deposited is necessary to obtain good adhesion and eliminate particle generation as well as to avoid trapping Cu contamination on the dielectric surface. Subtractive processes are needed in the back end of line for cleaning and bulk etching that both advance technology and minimize the discharge of heavy metals, such as copper, into waste streams.[3]

There is an extensive collection of literature on the deposition of Cu films by CVD using organometallic precursors. The most favorable precursor molecules are ligand-stabilized Cu(I) and Cu(II) β-diketonates,[4,5] which are fluorinated to increase volatility. Processes based on Cu(I) precursors generally yield higher deposition rates and do not require a carrier gas, and the lower oxidation state produces lower decomposition temperatures. Deposition of solid Cu(0) metal from Cu(I) hexafluoroacetylacetonate precursors occurs by a thermally induced disproportionation reaction

$$2(\mathrm{hfac})\mathrm{Cu^{I}L(g)} \rightleftharpoons \mathrm{Cu^{0}(s)} + \mathrm{Cu^{II}(hfac)_2} + 2\mathrm{L} \qquad (1)$$

where L is a Lewis base such as a triorganophosphine, olefin, or alkyne. At surface temperatures of 150−550 °C the deposition rate is typically on the order of 0.1 μm/min.[4]

* Corresponding author. E-mail: muscat@erc.arizona.edu.

(1) Steinbrüchel, C.; Chin, B. L. *Copper Interconnect Technology, Tutorial Texts in Optical Engineering*; SPIE: Bellingham, WA, 2001; Vol. TT46.
(2) Wolf, S.; Tauber, R. N. *Silicon Processing for the VLSI Era*, 2nd ed.; Lattice Press: Sunset Beach, CA, 2000; Vol. 1.
(3) Mendicino, L.; Brown, P. T. *Semicond. Int.* **1998**, *21* (6), 105.
(4) Hampden-Smith, M. J.; Kodas, T. T. Chemical vapor deposition of copper from Cu(I) compounds. In *The Chemistry of Metal CVD*; Hampden-Smith, M. J., Kodas, T. T., Eds.; VCH: Weinhiem, 1994.
(5) Griffin, G. L.; Maverick, A. W. CVD of copper from Cu(II) precursors. In *The Chemistry of Metal CVD*; Hampden-Smith, M. J., Kodas, T. T., Eds.; VCH: Weinhiem, 1994.

10.1021/cm048111a CCC: $30.25
Published on Web 03/11/2005

Cu(II) precursors generally have higher vapor pressures and undergo deposition reactions that are enhanced by water vapor.[6−9] Pyrolytic laser induced CVD of a hexafluoroacetylacetonate trimethylvinylsilane Cu(II) precursor in the presence of water vapor produced high-purity Cu lines at a growth rate of 1.8 μm/min, but under anhydrous conditions the growth rate was low and large amounts of carbon were incorporated.[10]

Chemistries using the organic acid hexafluoroacetylacetone (hfacH) can alternatively be used to dry etch Cu at much lower temperatures than are required for deposition. These dry etching processes are isotropic or nondirectional and have been proposed for cleaning the backside of wafers and CVD reactors that have been exposed to Cu. One approach is to reverse the CVD reaction (1) by reacting Cu metal with $Cu(hfac)_2$ and a Lewis base. Various Lewis bases have been shown to promote etching but the rates are less than 0.1 μm/min at 120−140 °C,[11] which is an order of magnitude lower than the approximately 1 μm/min typically needed for industrially viable dry etching processes. A more successful approach is to oxidize the Cu metal first and then react the nonvolatile metal oxide oligomers with an organic acid such as hfacH to form a volatile product.

Gas-phase Cl_2, O_2, O_3, and H_2O_2 have been used to oxidize Cu metal either prior or during exposure to hfacH. Jain *et al.* etched Cu metal at rates as high as 1 μm/min at 190 °C and 5 Torr using a continuous gas flow of approximately 1:4 hfacH to H_2O_2.[12] They found that at 200 °C the film was primarily Cu(I) oxide (Cu_2O), whereas at 250 °C the film was primarily Cu(II) oxide (CuO). Steger and Masel also achieved high Cu etching rates of approximately 1.65 μm/min using a continuous flow of 50 Torr hfacH and 200 Torr O_2, but the temperature and pressure were much higher, 350 °C and 250 Torr, respectively.[13] Decreasing both the temperature to 300 °C and the pressure below 200 Torr to ensure high mass transport, however, reduced the etching rate to approximately 0.2 μm/min. Nigg and Masel showed using temperature programmed desorption that oxygen preadsorbed on Cu(210) produced $Cu(hfac)_2$ at 150 °C after hfacH exposure and prevented polymerization of hfacH on the surface.[14] Kang *et al*. used O_3 gas and downstream O_2 and O_3 plasmas to oxidize Cu metal and found that the ratio of Cu(II) to Cu(I) oxide increased with temperature from 125 to 250 °C and plasma power.[15] The etching rate increased from 0.02 to 0.14 μm/min over this temperature range at a total reactor pressure of 0.9 Torr using a continuous flow of 1:8 hfacH to O_2 containing 5 vol % O_3. George *et al.* separated the oxidation and removal steps to investigate using hfacH as a chemical vapor clean for Cu.[16] Cu(I) and Cu(II) oxides were prepared by furnace oxidation of Cu metal and cleaned to remove adventitious carbon in a downstream plasma. The Cu oxides were removed by a 5 min exposure to a gas phase containing 2.5 Torr hfacH in a 7.5 Torr N_2 carrier but only when the temperature was raised above 200 °C. At lower temperatures, the oxidation state of the Cu was unchanged and no Cu oxides were removed when exposed to hfacH. The nominal etching rate was approximately 0.04 μm/min, which is sufficient for an industrial cleaning step in which a submonolayer surface coverage of Cu must be removed.

The processes used to fabricate metal wires in the manufacture of integrated circuits require large volumes of liquid chemicals and solvents since the same sequence of steps must be repeated for every metal level in the device. Utilizing supercritical CO_2 as a solvent offers a means to minimize the environment, safety, and health risks of processing because CO_2 is nontoxic and nonflammable and because gaseous CO_2 is readily separated from dissolved precursors, chelators, and other chemical additives and products that have much lower vapor pressures. There are technological advantages to replacing organic solvents with CO_2, which have been demonstrated for a variety of processes including chemical synthesis,[17−19] dry cleaning of clothing,[20] extractions,[21,22] separations,[23−25] emulsions,[26,27] and dispersions,[28] as well as applications such as patterning,[29] removing photoresist,[30] and drying to prevent pattern collapse[31] in the semiconductor industry. These processes are

(6) Kim, J.-Y.; Lee, Y.-K.; Park, H.-S.; Park, J.-W.; Park, D.-K.; Joo, J.-H.; Lee, W.-H.; Ko, Y.-K.; Reucroft, P. J.; Cho, B.-R. *Thin Solid Films* **1998**, *330*, 190.
(7) Pinkas, J.; Huffman, J. C.; Baxter, D. V.; Chisholm, M. H.; Caulton, K. G. *Chem. Mater.* **1995**, *7*, 1589.
(8) Lecohier, B.; Philippoz, J.-M.; Calpini, B.; Stumm, T.; van den Bergh, H. *J. Phys. (Paris) IV* **1991**, *C2*, 279.
(9) Lecohier, B.; Philippoz, J.-M.; Calpini, B.; Stumm, T.; van den Bergh, H. *J. Appl. Phys.* **1992**, *72* (5), 2022.
(10) Widmer, M.; van den Bergh, H. *J. Appl. Phys.* **1995**, *77* (10), 5464.
(11) Hampden-Smith, M. J.; Kodas, T. T. *MRS Bull.* **1993**, *13* (6), 39.
(12) Jain, A.; Kodas, T. T.; Hampden-Smith, M. J. *Thin Solid Films* **1995**, *269*, 51.
(13) Steger, R.; Masel, R. *Thin Solid Films* **1999**, *342*, 221.
(14) Nigg, H. L.; Masel, R. I. *Surf. Sci.* **1998**, *409*, 428.
(15) Kang, S.-W.; Kim, H.-U.; Rhee, S.-W. *J. Vac. Sci. Technol. B* **1999**, *17* (1), 154.
(16) George, M. A.; Hess, D. W.; Beck, S. E.; Ivankovits, J. C.; Bohling, D. A.; Felker, B. S.; Lane, A. P. Reaction of 1,1,1,5,5,5-hexafluoro-2,4-pentanedione (hfac) with surfaces of CuO, Cu_2O, and Cu studied by XPS. In *Proceedings of the 3rd International Symposium on Cleaning Technology in Semiconductor Device Manufacturing*; Ruzyllo, J., Novak, R. E., Eds.; Electrochemical Society Proceedings: 1994; Vol. 94-7, p 272.
(17) Mera, A. E.; Morris, R. E. *Macromol. Rapid Commun.* **2001**, *22* (7), 513.
(18) Ke, J.; Han, B.; George, M. W.; Yan, H.; Poliakoff, M. *J. Am. Chem. Soc.* **2001**, *123* (16), 3661.
(19) Pai, R. A.; Humayun, R.; Schulberg, M. T.; Sengupta, A.; Sun, J.-N.; Watkins, J. J. *Science* **2004**, *303*, 507.
(20) McClain, J. B.; Betts, D. E.; Canelas, D. A.; Samulski, E. T.; DeSimone, J. M.; Londono, J. D.; Cochran, H. D.; Wignall, G. D.; Chillura-Martino, D.; Triolo, R. *Science* **1996**, *274*, 2049.
(21) Vasapollo, G.; Longo, L.; Rescio, L.; Ciurlia, L. *J. Supercrit. Fluids* **2004**, *29* (1−2), 87.
(22) Ohashi, K.; Tatenuma, K. *Chem. Lett.* **1997**, *11*, 1135.
(23) Gamlieli-Bonshtein, I.; Korin, E.; Cohen, S. *Biotechnol. Bioeng.* **2002**, *80* (2), 169.
(24) Matsuyama, H.; Yamamoto, A.; Yano, H.; Maki, T.; Teramoto, M.; Mishima, K.; Matsuyama, K. *J. Membr. Sci.* **2002**, *204* (1−2), 81.
(25) Eckert, C. A.; Bush, D.; Brown, J. S.; Liotta, C. L. *Ind. Eng. Chem. Res.* **2000**, *39* (12), 4615.
(26) Dickson, J. L.; Binks, B. P.; Johnston, K. P. *Langmuir* **2004**, *20* (19), 7976.
(27) Johnston, K. P.; Lee, C. T.; Li, G.; Psathas, P.; Holmes, J. D.; Jacobson, G. B.; Yates, M. Z. *Surf. Sci. Ser.* **2001**, *100* (Reactions and Synthesis in Surfactant Systems), 349.
(28) Dickson, J. L.; Shah, P. S.; Binks, B. P.; Johnston, K. P. *Langmuir* **2004**, *20* (21), 9380.
(29) Pryce-Lewis, H. G.; Weibel, G. L.; Ober, C. K.; Gleason, K. K. *Chem. Vap. Deposition* **2001**, *7* (5), 195.
(30) Chavez, K. L.; Bakker, G. L.; Hess, D. W. *J. Vac. Sci. Technol. B* **2001**, *19*, 2144.
(31) Goldfarb, D. L.; Pable, J. J.; Nealey, P. F.; Simons, J. P.; Moreau, W. M.; Angelopoules, M. *J. Vac. Sci. Technol. B* **2000**, *18*, 3313.

possible because supercritical CO_2 is a nonaqueous fluid with good mass transport properties and a tunable solvent strength, low surface tension, and a liquidlike density.

Metal films have been deposited and etched using supercritical CO_2. Blackburn *et al.* deposited Cu on metal and metal oxide surfaces seeded with clusters of Pd by hydrogen reduction of Cu(II) β-diketonates including $Cu(hfac)_2$ dissolved in $scCO_2$ at 175−200 °C and 200 atm.[32] They also demonstrated that high-purity Cu films could be deposited using Cu(I) precursors by the disproportionation reaction (1) onto SiO_2 and metal diffusion barriers such as TiN by hydrogen-assisted reduction at 225 °C and 200 atm. Below 200 °C the deposition was found to be selective for metal surfaces over SiO_2. The use of nonfluorinated precursors is desirable because of disposal issues and both Cu(I) and Cu(II) organometallic precursors were shown to yield similar results as that for $Cu(hfac)_2$. Ohde *et al.* demonstrated that adding a homogeneous Pd catalyst to a $scCO_2$ mixture lowered the deposition temperature of high-quality Cu films to 100 °C on Ta and other barrier metals by the hydrogen reduction of $Cu(hfac)_2$.[33] Douglas and Templeton have been issued two patents describing in general terms the removal of metal atoms from wafer surfaces using a chelator dissolved in $scCO_2$.[34,35] Bessel *et al.* demonstrated that Cu coupons were etched in a mixture of the oxidant ethyl peroxydicarbonate and different β-diketonate chelating molecules dissolved in $scCO_2$ at 40 °C and 214 bar.[36] The effort was directed at developing a $scCO_2$-based CMP process. They found that the removal rate using hfacH was 158 layers of Cu/min or approximately a factor of 3 times greater than with chelators containing less fluorine, which they attribute to solubility of the Cu-bearing complexes in CO_2.

The goal of this work is to demonstrate a proof of concept process for the removal of Cu metal from a silicon surface using hfacH dissolved in $scCO_2$. Silicon was chosen for study rather than a dielectric film because Cu deposition from solution required a conductive surface. Copper islands with nominal concentrations on the order of 10^{16} atoms/cm^2 were chosen for study since this range is most relevant for wafer surface cleaning applications in the semiconductor industry. A two-step process of oxidation and etching with hfacH dissolved in $scCO_2$ removed Cu on Si to the detection limit of X-ray photoelectron spectroscopy (XPS) and removed Cu islands in SEM images. The morphology of Cu(II)O formed by exposure to liquid H_2O_2 had a flake appearance and could be etched selectively to $Cu(I)_2O$ by releasing the reactor pressure at a rate of 300 atm/min. Both Cu(II)O and $Cu(I)_2O$ as well as Cu chlorides were removed chemically using hfacH dissolved in $scCO_2$. The removal of Cu(I)O is proposed to occur via oxidation by a byproduct of Cu(II) etching and subsequent attack of Cu(II) by hfacH.

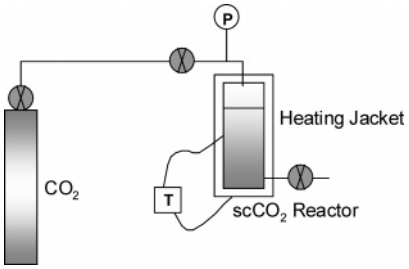

Figure 1. Schematic of the supercritical CO_2 reactor system. After loading, the reactor was chilled to 8 °C and fed with liquid CO_2 to approximately 60 atm. The cylinder was valved off and the reactor was heated using a heating jacket and setpoint controller until the desired steady-state conditions were reached. After processing, the fluid was exhausted through a needle valve.

Experimental Section

Samples contaminated with Cu were prepared by immersing silicon pieces in an HF solution doped with copper sulfate. Four-inch p-type Si(100) wafers (resistivity 0.001−0.02 Ω-cm) were cleaved into 1.5 × 1.5 cm^2 pieces and cleaned immediately prior to Cu deposition using a three-step process, consisting of a 49% HF dip for 5 min, followed by piranha (5:1 by volume H_2SO_4:H_2O_2 heated to 150 °C) for 5 min, and a 49% HF last step for 5 min. Solutions containing 20 ppm of copper ions were prepared using copper sulfate ($CuSO_4 \cdot 5H_2O$) dissolved in 5% aqueous HF at 19 °C. Silicon samples were allowed to lay flat in a beaker containing the Cu/HF solution under illumination from a fluorescent lamp to achieve a uniform Cu coverage on the surface[37] from the photocatalyzed adsorption reaction.[38] Samples were rinsed in ultrapure water (18 MΩ-cm) for 10 s and blown dry with N_2 (liquid boiloff). Sample preparation using this procedure has been shown to produce copper islands or clusters on the surface,[37,39] which was verified with scanning electron microscopy (SEM) images taken with an Hitachi S-4500 field emission microscope and atomic force microscopy (AFM) recorded with a Digital Instruments, Inc. MM-AFM-1 (multimode) Nanoscope III in tapping mode.

After Cu contamination, some samples were oxidized using one of two different procedures. Gas-phase oxidation with chlorine was accomplished by processing a sample for 35 min at 50 °C and 1 Torr total pressure in a 10% Cl_2 (Air Products & Chemicals, Inc., VLSI grade, 99.998%) gas flow diluted with N_2 under direct illumination from a 1000-W Xe arc lamp. Liquid-phase oxidation was accomplished by processing a sample for up to 10 min at room temperature in a 30% aqueous H_2O_2 solution (Ashland Chemical, Cleanroom Electronic Grade), rinsing with isopropyl alcohol (IPA), and blowing dry with N_2.

The experimental $scCO_2$ system used to process samples consisted of a stainless steel reactor fed by a liquid CO_2 bottle (Figure 1). The reactor was constructed from two cylindrical pieces of $^1/_2$-in. wall 316 stainless steel that screwed together and sealed over a 1-in. diameter seat fitted with a Urethane-70 O-ring in the upper piece. The reactor inner diameter was 1 in. and the total volume was approximately 200 cm^3. The two pieces were taken apart each time to remove and load samples and chemicals. Samples

(32) Blackburn, J. M.; Long, D. P.; Cabañas, A.; Watkins, J. J. *Science* **2001**, *294*, 141.
(33) Ohde, H.; Kramer, S.; Moore, S.; Wai, C. M. *Chem. Mater.* **2004**, *16*, 4028.
(34) Douglas, M. A.; Templeton, A. C. Method for removing inorganic contamination by chemical derivatization and extraction. Patent No. 5,868,856, 1999.
(35) Douglas, M. A.; Templeton, A. C. Method of removing inorganic contamination by chemical alteration and extraction in a supercritical fluid media. Patent No. 5,868,862, 1999.
(36) Bessel, C. A.; Denison, G. M.; DeSimone, J. M.; DeYoung, J.; Gross, S. M.; Schauer, C. K.; Visintin, P. M. *J. Am. Chem. Soc.* **2003**, *125*, 4980.
(37) Lee, M. K.; Wang, J. J.; Wang, H. D. *J. Electrochem. Soc.* **1997**, *144* (5), 1777.
(38) Teerlinck, I.; Mertens, P. W.; Schmidt, H. F.; Meuris, M.; Heyns, M. M. *J. Electrochem. Soc.* **1996**, *143* (10), 3323.
(39) Li, G.; Jiao, J.; Seraphin, S.; Raghavan, S.; Jeon, J. S. *J. Appl. Phys.* **1999**, *85* (3), 1857.

Table 1. Bulk Copper XPS Binding Energies as a Function of Oxidation State (Values in Parentheses Were Calculated Based on $2p_{3/2}$ Shift)[42,60]

binding energy, eV	Cu oxidation state				
spin−orbit coupling	$Cu(II)Cl_2$	Cu(II)O	Cu(0) metal	Cu(I)Cl	$Cu(I)_2O$
$2p_{3/2}$	934.5	933.6	932.7	932.4	932.4
$2p_{3/2}$ satellite	943	943			
$2p_{1/2}$	(954.3)	(953.4)	952.5	(952.2)	(952.2)
$2p_{1/2}$ satellite	963	962.5			

were placed upright on the bottom of the reactor with the top edge leaning against the reactor wall; samples were not held in place by mounting hardware. The polished side of the sample used for analysis was faced toward the reactor wall. The chelating agent used to investigate the complexation of Cu was 1,1,1,5,5,5-hexafluoro-2,4-pentanedione or hexafluoroacetylacetone (hfacH) (Alfa Aesar, 99.4%). A disposable syringe (1-mL total volume) was used to put 0.05 mL of hfacH into the recess created by the lower exhaust port at the bottom of the reactor. This amount of hfacH produced a concentration during an experiment of approximately 120 ppm on a molar basis. There was no direct contact between the hfacH and sample during loading.

After the upper cylinder was screwed onto the lower cylinder, the reactor was cooled to 8 °C in an ice bath and charged with liquid CO_2 (99.5%) to approximately 60 atm through $^1/_4$-in. stainless steel tubing. The air in the reactor could not be purged before filling with liquid CO_2 without allowing hfacH to escape from the lower exhaust port; consequently, all experiments also include approximately 200 cm^3 of ambient air at 23 °C. During filling the liquid level likely rose above the sample on the bottom of the reactor since Si has a higher density than CO_2; however, there was no sight glass on the reactor to visually verify the level. After charging, the reactor was heated and required approximately 12 min to cross into the supercritical CO_2 region, which typically occurred at 31 °C and approximately 150 atm, and another 3 min to reach steady state at the desired processing temperature and pressure. Processing times include only the time spent at steady-state conditions and do not include the approximately 15-min ramp. The resistively heated jacket and insulation covering the reactor allowed a temperature setpoint to be reached within ±5 °C using a thermocouple and controller. Pressure was read using a Bourdon tube with an accuracy of ±20 psi (±1.4 atm) in the range 0−5000 psi. Since precise control over the final reactor temperature and pressure was not possible with this system, fluid densities computed using the Peng−Robinson equation of state are noted for comparison. The parameter ranges studied include temperature from 40 to 60 °C and pressure from 100 to 250 atm, producing densities between 0.5 and 0.75 g/cm^3. All experiments were run as batch processes using the same procedure. After processing, the reactor pressure was released through a $^1/_4$-in. needle valve either quickly in the majority of experiments reaching ambient in less than 1 min (fast release) or slowly in one set of experiments reaching ambient in approximately 5 min (slow release).

Surface characterization of Cu and other species on the wafer surface was done ex situ using an X-ray photoelectron spectrometer (Physical Electronics, Model 549) with a double-pass cylindrical mirror analyzer and a 400-W X-ray gun (Mg Kα radiation, 1253.6 eV). Approximately 15 XPS spectra were co-added for each pre- and postprocess characterization. Peak assignments for Cu are summarized in Table 1. Cu removal on the surface was obtained by referencing the area under the Cu $2p_{3/2}$ peak envelope to the area under the Si 2p peak envelope both before and after processing to obtain the percent change defined by

$$\{\text{Change in referenced Cu peak area}\} = \frac{\left\{\frac{\text{Initial Cu Area}}{\text{Initial Si Area}}\right\} - \left\{\frac{\text{Final Cu Area}}{\text{Final Si Area}}\right\}}{\left\{\frac{\text{Initial Cu Area}}{\text{Initial Si Area}}\right\}} \quad (2)$$

Positive changes are indicative of Cu removal, and negative changes indicate that the surface was contaminated with adsorbed hfacH molecules, which attenuated the Si signal more than the Cu signal.

Results

Copper Deposition Morphology and Oxidation State. Figure 2a shows a high-resolution SEM image of a Si surface after contamination using a Cu-doped aqueous HF solution. The Cu deposited in hexagonal-shaped islands that were at the center of etching pits created in the Si surface during deposition. Cu island and pit formation have been observed previously using aqueous HF solutions and are the result of a reduction−oxidation (redox) reaction between a Cu ion and the Si surface producing Cu(0) metal deposits and Si oxide which is subsequently etched by HF.[40] Previous work by Ohmi's group has shown that pitting is not a function of dopant type or concentration. The diameters of the Cu islands observed in SEM images ranged in size from 10 to 90 nm. AFM was used to confirm the SEM results and in addition showed that the approximate height of the islands was 20 nm with an overall surface RMS roughness value of 3.9 nm. With use of a cylinder that is half as high as it is wide to model the shape of a Cu island and assuming that the islands had a density equal to that of bulk Cu metal, analysis of SEM pictures from four separate 0.8×1.1 μm areas on the same Si sample yielded a coverage of 5−25 Cu atoms per Si surface atom or 7×10^{15} to 3×10^{16} atoms/cm^2.

XPS was used to determine the oxidation state and the chemical composition of the Cu deposits. XPS peaks in the Cu 2p range at binding energies of 932.7 and 952.5 eV were observed for Cu-contaminated Si as shown for a representative sample in Figure 3a. The Cu 2p XPS binding energies summarized in Table 1 indicate that the deposition from HF solution yielded either Cu(0) metal or Cu(I), but not Cu(II), since the satellite peaks and shoulders on the $2p_{1/2}$ and $2p_{3/2}$ states, which are indicative of Cu(II), are missing. The Cu oxidation state cannot be completely resolved based on the 2p XPS data because the Cu(0) metal and Cu(I) peaks overlap. Auger spectra for the Cu($L_3M_{4,5}M_{4,5}$) transition, which is induced by X-ray exposure, were used instead to discriminate between Cu(0) metal and Cu(I). The binding energies for X-ray-induced Cu Auger peaks are summarized in Table 2. The peak assignments made in Table 2 are shifted to higher binding energy by approximately 0.2−0.8 eV compared to the literature values but the ordering of the oxidation states is the same.[41,42] The Cu($L_3M_{4,5}M_{4,5}$) Auger transition of a Cu-contaminated Si sample (as contaminated sample) is a single peak located at a binding energy of 337.3

(40) Morinaga, H.; Suyama, M.; Ohmi, T. *J. Electrochem. Soc.* **1994**, *141* (10), 2834.
(41) Chawla, S. K.; Sankarraman, N.; Payer, J. H. *J. Electron Spectrosc. Relat. Phenom.* **1992**, *61* (1), 1.
(42) Klein, J. C.; Proctor, A.; Hercules, D. M.; Black, J. F. *Anal. Chem.* **1983**, *55*, 2055.

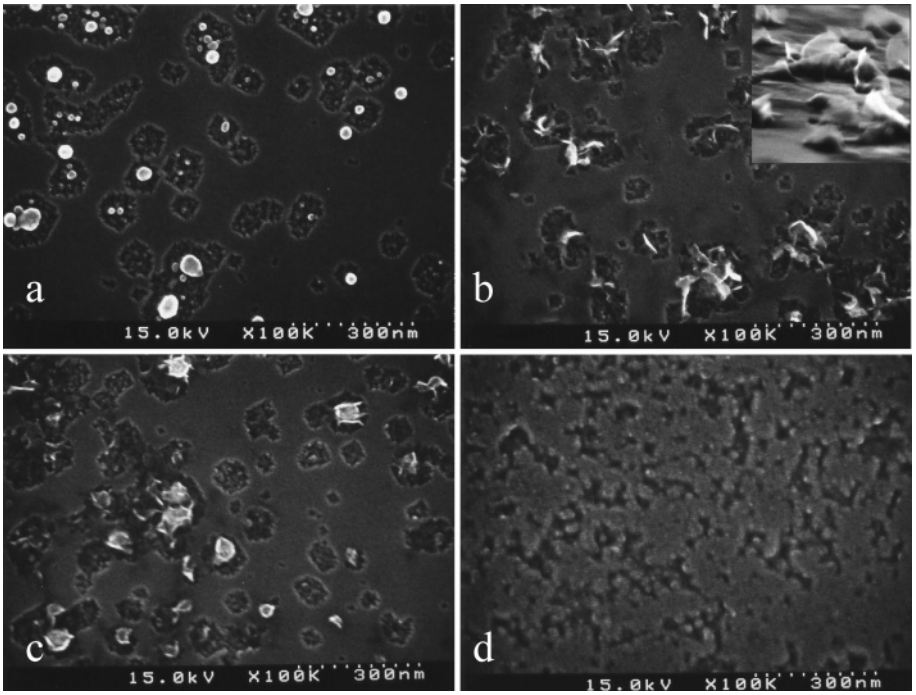

Figure 2. SEM images of different 0.8 × 1.1 μm areas of Si (100 orientation, p-type 0.001−0.02 Ω-cm) samples after the following processes. (a) Cu deposition from aqueous 5% HF solution doped with 20 ppm Cu for 5 min (as-contaminated Si sample). (b) Oxidation in 30% H_2O_2 for 5 min at 19 °C. The inset is a side view SEM image showing flake structure. (c) Exposure of oxidized Cu-contaminated Si sample to pure $scCO_2$ at 49 °C and 225 atm for 5 min. (d) Exposure of oxidized Cu-contaminated Si sample to $scCO_2$ containing 120 ppm hfacH at 59 °C and 170 atm for 5 min and fast pressure release. Magnification of 100 000× was used to collect all images.

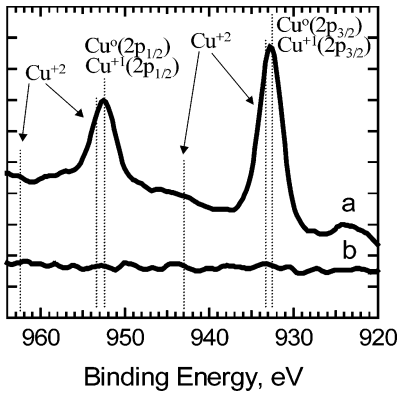

Figure 3. (a) XPS spectrum in the Cu 2p energy range of a Si surface after immersion for 5 min in 5% HF doped with 20 ppm Cu (as-contaminated Si sample). (b) XPS spectrum after exposing as-contaminated sample in (a) to 30 min of pure liquid hfacH in air at 19 °C followed by an isopropyl alcohol rinse. The Cu(0) metal and Cu(I) states overlap, producing $2p_{3/2}$ and $2p_{1/2}$ envelopes at binding energies of 932.7 and 952.5 eV, respectively. The Cu(II) $2p_{3/2}$ and $2p_{1/2}$ peaks at 933.6 and 953.4 eV, respectively, appear as shoulders on the Cu(0) and Cu(I) peak envelopes. Cu(II) is best distinguished by $2p_{3/2}$ and $2p_{1/2}$ shake-up satellites at 943 and 962.5 eV, respectively.

Table 2. Cu($L_3M_{4,5}M_{4,5}$) Auger Transitions Induced by X-ray Exposure as a Function of Oxidation State

	Cu oxidation state		
binding energy, eV	Cu(I)	Cu(II)	Cu(0) metal
$L_3M_{4,5}M_{4,5}$	337.3	336	335

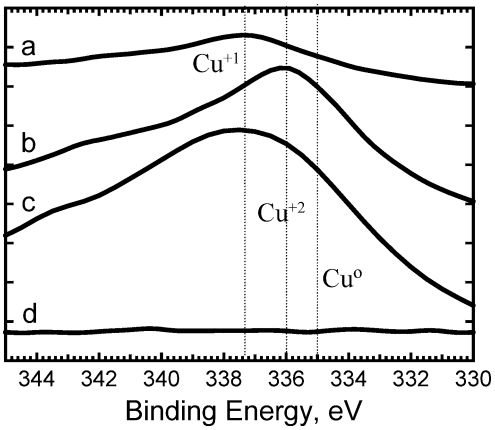

Figure 4. Cu($L_3M_{4,5}M_{4,5}$) Auger spectra induced by X-ray exposure. (a) Cu-contaminated Si sample; (b) Cu-contaminated Si sample oxidized for 10 min in aqueous 30% H_2O_2; (c) after exposure of sample in (b) to a 15 min ramp to steady-state conditions followed by a 2 min $scCO_2$ process at 55 °C and 165 atm (0.59 g/cm^3) and rapid pressure release (~300 atm/min); (d) after exposure of sample in (b) to a mixture of $scCO_2$ and hfacH (0.05 mL or 120 ppm) to a 15 min ramp to steady-state conditions followed by a 5 min $scCO_2$ process at 54 °C and 151 atm (0.63 g/cm^3).

eV as shown in Figure 4a. This state is indicative of Cu(I) formation. These results demonstrate that, in the near surface region probed by XPS, the initial Cu deposit contained $Cu(I)_2O$. This oxide was likely formed after deposition during exposure of metallic Cu deposits to air.

Oxidizing the samples intentionally changed both the morphology of the Cu islands as well as the Cu oxidation state. Figure 2b shows a SEM image after oxidation of a Cu-contaminated Si sample in 30% H_2O_2 for 5 min at 19 °C. The bright structures imaged by SEM near the centers of the etching pits were no longer hexagonal, but were flattened and appeared to be oriented perpendicular to the surface. The off-normal SEM (inset Figure 2b) shows that the structures were irregularly shaped flakes. Consistent with a change in the vertical profile of the islands, the surface roughness measured by AFM increased to 7.5 nm. Note that the Si surface was oxidized to SiO_2 by H_2O_2. XPS analysis of oxidized samples in the Cu 2p range contained new peaks at binding energies of 943 and 962.5 eV (Figure 5a), which are indicative of Cu(II)O (Table 1). The Cu(II) $2p_{1/2}$ and $2p_{3/2}$

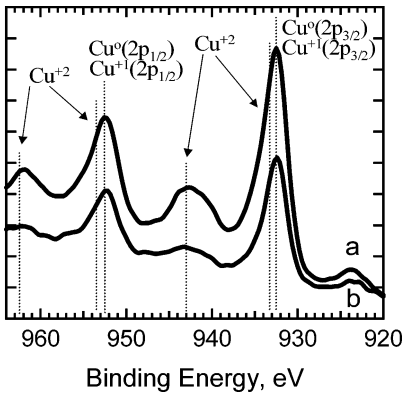

Figure 5. Oxidized Cu and $scCO_2$ experiment. (a) XPS spectrum in the Cu 2p binding energy range of a Cu-contaminated Si sample oxidized for 10 min in a 30% H_2O_2 solution. The $2p_{3/2}$ satellite peak is prominent at approximately 943 eV, indicating that Cu(II) oxide (CuO) formed; (b) XPS spectrum after exposing sample in (a) to a 15 min ramp to steady-state conditions and a 3 min $scCO_2$ process at 56 °C and 156 atm (0.63 g/cm^3).

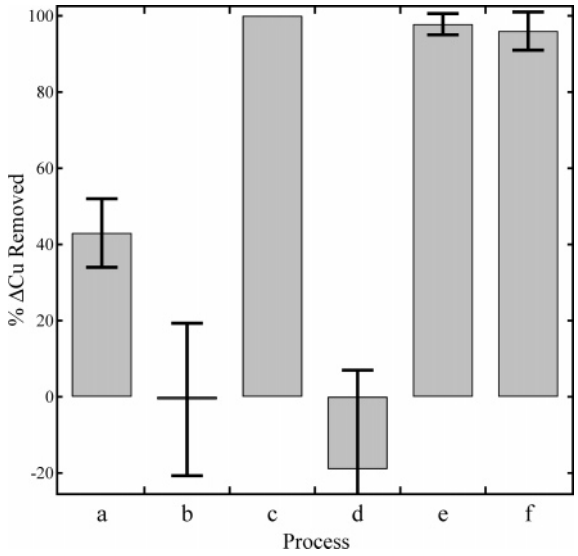

Figure 6. Summary of the mean changes in the referenced Cu XPS peak areas computed using eq 2 as a function of the processes listed in Table 3. Error bars define 95% confidence intervals.

peaks expected at 933.6 and 953.4 eV, respectively, appear as shoulders on the Cu(I)/Cu(0) peak envelope. The X-ray induced Cu($L_3M_{4,5}M_{4,5}$) Auger transition broadened and shifted to 336 eV (Figure 4b) after oxidation with H_2O_2, which is consistent with the formation of Cu(II)O (Table 2). The peak shape and energy of the Cu(II) oxide Auger peak in Figure 4b is similar to literature values reported for sputter-deposited Cu films and pure Cu disks oxidized using H_2O_2 or O_2 gas at temperatures from 200 to 400 °C.[12,13] The aqueous H_2O_2 oxidation step converted only a portion of the Cu(I) into Cu(II), however, since peaks at binding energies of 932.7 and 952.5 eV were still evident in the XPS spectrum (Figure 5a). In principle, the width of the Cu(II) Auger peak could denote the presence of the other oxidation states; however, the peak width of the Cu Auger transition increases with the oxidation state, making the Cu(I) state difficult to resolve (Figure 4b).[43] Based on XPS and Auger spectra from several samples, approximately half of the $Cu(I)_2O$ was converted to Cu(II)O, suggesting that the aqueous oxidation reaction was self-limiting.

(43) Timmermans, B.; Reniers, F.; Hubin, A.; Buess-Herman, C. *Appl. Surf. Sci.* **1999**, *144−145*, 54.

Table 3. Summary of Processes Investigated for Cu Removal from Si (+, Used; −, Not Used; NA, Not Applicable)

process	oxidized	hfacH	$scCO_2$	$scCO_2$ rinse	fast release
a	+	−	+	−	+
b	+	−	+	−	−
c	−	+	NA	NA	NA
d	−	+	+	−	+
e	+	+	+	−	+
f	+	+	+	+	+

Copper Removal. The bar graph in Figure 6 summarizes the percentage of Cu removed from as-contaminated samples by various process sequences. Table 3 outlines the sequences investigated, which were comprised of one or more of five possible steps (indicated by +), including intentional oxidation of an as-contaminated sample, hfacH, $scCO_2$, $scCO_2$ rinse, and fast (+) or slow (−) release of the pressure in the reactor after $scCO_2$ processing. A +/+ hfacH and $scCO_2$ combination in Table 3 indicates that hfacH was dissolved in $scCO_2$. A −/+ hfacH/$scCO_2$ combination indicates that the sample was processed in pure $scCO_2$. The +/NA combination in process c means that pure hfacH was used in the cleanroom. The percent of Cu removed by each process sequence in the bar graph in Figure 6 is the average value computed using eq 2 based on pre- and post-XPS scans starting with freshly prepared samples for each experiment. The error bars shown are ±2 standard deviations or 95% confidence intervals.

A pure $scCO_2$ process removed approximately half of the Cu from oxidized as-contaminated samples. This is process "a" in Table 3 and Figure 6 and included oxidizing the sample, processing with $scCO_2$, and releasing the CO_2 pressure quickly. After a Si sample was contaminated with Cu, the wafer was dipped in an aqueous 30% H_2O_2 solution for 10 min, rinsed with IPA, and blown dry with N_2. The XPS spectrum indicated that Cu(II) oxide, CuO, formed as shown by the shake-up satellite peaks at 943 and 962.5 eV in Figure 5a. Processing the as-contaminated and oxidized sample for a 3-min soak in $scCO_2$ at 56 °C and 156 atm (0.63 g/cm^3) resulted in a 50% decrease in the Cu peak area (Figure 5b). Reference of the Cu to the Si 2p peak area using eq 2 allowed removal percentages to be compared across all processes without introducing artifacts caused by changes in other atomic constituents on the surface. The Cu(II) satellite peaks at 943 and 962.5 eV were reduced appreciably but some Cu(II)O remained on the sample. The Cu($L_3M_{4,5}M_{4,5}$) Auger transition shifted to higher binding energy as a result of $scCO_2$ processing, which shows that Cu(II) oxide was removed preferentially to Cu(I) (Figure 4c). The $Cu(I)_2O$ Auger peak centered at 337.3 eV was broad, however, which is consistent with the presence of Cu(II)O. A SEM image after fast pressure release shows that Cu islands were still present on the surface, but that most of the flakes were removed (Figure 2c). Flake structure is apparent around some of the large islands in the image. AFM analysis showed that the islands were flattened compared to the as-contaminated sample and that the RMS surface roughness of 4.5 nm was lower than when the flake structures were present.

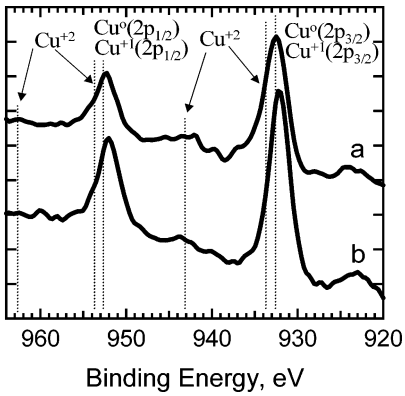

Figure 7. Nonoxidized/$scCO_2$ only experiment. (a) XPS spectrum in the Cu 2p energy range of a Cu-contaminated Si sample; (b) XPS spectrum after exposing sample in (a) to a 15 min ramp to steady-state conditions and a 3 min $scCO_2$ process at 55 °C and 150 atm (0.62 g/cm^3).

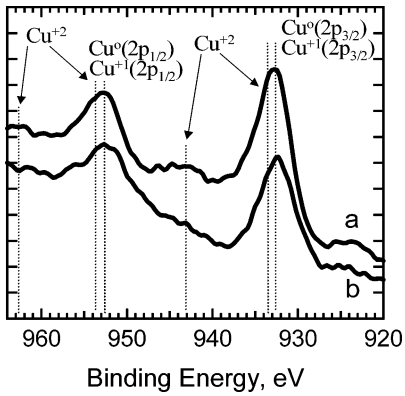

Figure 8. hfac/$scCO_2$ experiment. (a) XPS spectrum in the Cu 2p energy range of a Cu-contaminated Si sample; (b) XPS spectrum after adding 0.05 mL of hfacH to the reactor and exposing sample in (a) to a 15 min ramp to steady-state conditions followed by a 60 min $scCO_2$ process at 44 °C and 136 atm (0.68 g/cm^3).

The pressure in the reactor after $scCO_2$ processing in sequence "a" was released quickly to ambient conditions in less than 1 min to achieve a rate of approximately 300 atm/min. The rate of pressure release was essential to removing Cu(II)O. Process "b" in Table 3 and Figure 6 shows that Cu was not removed, on average, from oxidized samples when the release rate was approximately 30 atm/min or an order of magnitude slower compared to that of the fast release experiments. The large error bars were likely the result of releasing the system pressure through a needle valve, which was difficult to control reproducibly.

Releasing the reactor pressure rapidly after processing a nonoxidized sample with $scCO_2$ did not change the amount of Cu on the surface. Processing a sample containing only $Cu(I)_2O$ islands (as-contaminated sample) in $scCO_2$ for 3 min at 55 °C and 150 atm (0.62 g/cm^3) and releasing the pressure quickly resulted in a net change of −21% in the referenced Cu peak area calculated using eq 2. The pre- and postprocess XPS spectra are shown in Figure 7. The negative change was the result of the adsorption of adventitious C on the surface since the C 1s XPS peak also increased. These results demonstrate that processing in pure $scCO_2$ removed Cu(II)O selectively to $Cu(I)_2O$ when the system pressure was released quickly after the soak time.

In a proof of concept experiment, a sample was exposed to hfacH in ambient air to chemically remove Cu. A droplet containing 0.5 mL of pure hfacH was placed on the surface of an as-contaminated sample using a plastic bulb in a chemical hood in the cleanroom. After 30 min at 19 °C the surface was rinsed with IPA and blown dry with N_2. Pre- and postprocess XPS spectra of the sample in the Cu $2p_{1/2}$ and $2p_{3/2}$ binding energy range show that Cu was completely removed from the surface to the detection limit of XPS (Figure 3). Rinsing an as-contaminated sample with IPA and blowing dry with N_2 did not change the Cu XPS spectrum, indicating that pure hfacH in air completely removed Cu from the surface. The complete removal of Cu by pure hfacH in air is process "c" in Table 3 and Figure 6.

In contrast to the cleanroom experiment in air at ambient conditions, dissolving hfacH in $scCO_2$ did not remove Cu from the surface of as-contaminated samples (process "d" in Table 3 and Figure 6). Processing an as-contaminated sample in $scCO_2$ containing 120 ppm hfacH at 44 °C and 136 atm (0.68 g/cm^3) for 60 min resulted in a −46% change in the percentage of Cu removed. Copper was not added to the surface; rather the negative change indicates that another species, in this case hfacH, adsorbed on the surface, since both the C and F XPS peaks increased. The attenuation of the Cu $2p_{3/2}$ peak envelope in the pre- and postprocess spectra shown in Figure 8 was less than that for the Si 2p peaks, which explains the sign and magnitude of the change. Judging from the satellite peak at 943 eV, the small amount of Cu(II) present initially appears to have been removed. The hfacH concentration was approximately 120 ppm. Air was not purged from the reactor so it was present during processing. The concentrations of both hfacH and air during supercritical fluid processing in the reactor were much lower than those in the experiment in the cleanroom.

Oxidizing as-contaminated samples followed by processing in a mixture of hfacH dissolved in $scCO_2$ removed all of the copper from the surface (processes "e" and "f" in Table 3 and Figure 6). Both a UV−Cl_2 gas phase and an aqueous H_2O_2 solution were used as oxidants with identical results. Exposing an as-contaminated sample to UV−Cl_2 at 50 °C converted a portion of the $Cu(I)_2O$ to Cu(II) chloride ($CuCl_2$) on the surface (Figure 9a). Following this step with 120 ppm of hfacH dissolved in $scCO_2$ at 58 °C and 180 atm (0.67 g/cm^3) for a soak time of 5 min removed all Cu on the surface to below the XPS detection limit (Figure 9b). Both the C and F XPS peaks increased, however. Oxidizing the surface instead with an aqueous 30% H_2O_2 solution for 5 min and processing in hfacH dissolved in $scCO_2$ at 49 °C and 138 atm (0.63 g/cm^3) for 2 min followed by a pure $scCO_2$ exposure to rinse the surface not only removed Cu (Figure 10) but also kept the C and F coverages unchanged from the initial preprocess levels (Figure 11). A separate experiment using aqueous H_2O_2 as an oxidant without rinsing removed Cu completely, but the C and F peaks increased. The Cu($L_3M_{4,5}M_{4,5}$) Auger data corroborates the XPS results as the Cu transitions disappeared after processing an oxidized sample in hfacH and $scCO_2$ (Figure 4d). Moreover, a SEM image showed that all of the Cu islands and flake structures were removed, leaving only etching pits on the surface (Figure 2d). These results indicate that an oxidant is necessary to completely remove Cu with hfacH and that

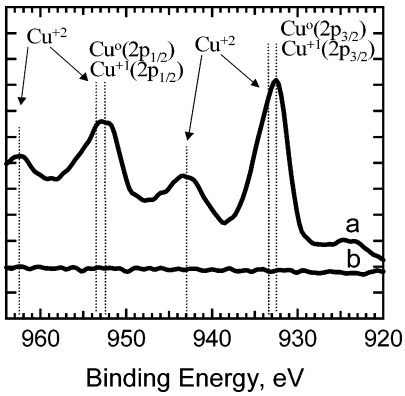

Figure 9. Oxidized with Cl_2 and hfacH/$scCO_2$ clean experiment. (a) XPS spectrum in the Cu 2p energy range of a Cu-contaminated Si sample oxidized for 35 min in UV−Cl_2 at 10 mTorr and 50 °C. (b) XPS spectrum after adding 0.05 mL of hfacH to the reactor and exposing sample in (a) to a 15 min ramp to steady-state conditions followed by a 5 min $scCO_2$ process at 58 °C and 180 atm (0.67 g/cm^3).

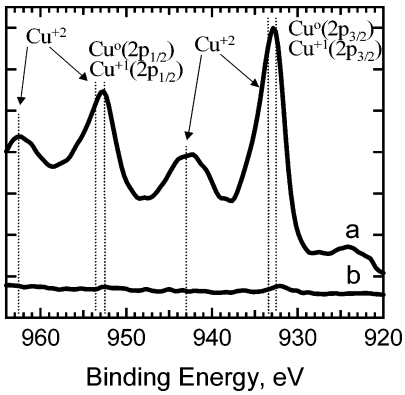

Figure 10. Oxidized with H_2O_2 and hfacH/$scCO_2$ clean plus $scCO_2$ rinse experiment. (a) XPS spectrum in the Cu 2p energy range of a Cu-contaminated Si sample oxidized for 5 min in aqueous 30% H_2O_2. (b) XPS spectrum after adding 0.05 mL of hfacH to the reactor and exposing sample in (a) to a 15 min ramp to steady-state conditions followed by a 2 min $scCO_2$ process at 49 °C and 138 atm (0.63 g/cm^3). After evacuation of the reactor, a pure $scCO_2$ process was run to rinse the sample.

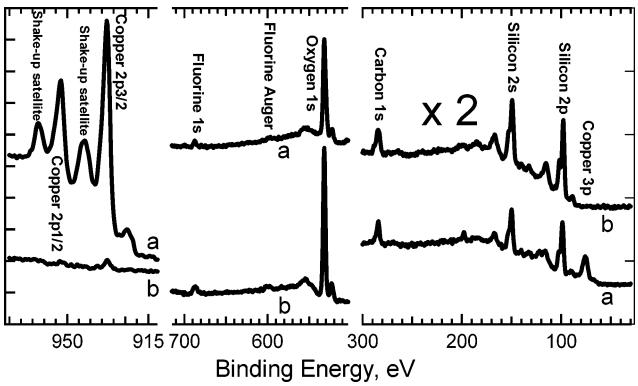

Figure 11. Oxidized with H_2O_2 and hfacH/$scCO_2$ clean plus $scCO_2$ rinse experiment. (a) XPS spectrum of a Cu-contaminated Si sample oxidized for 5 min in aqueous 30% H_2O_2. (b) XPS spectrum after adding 0.05 mL of hfacH to the reactor and exposing sample in (a) to a 15 min ramp to steady-state conditions followed by a 2 min $scCO_2$ process at 49 °C and 138 atm (0.63 g/cm^3). After evacuation of the reactor, a pure $scCO_2$ process was run to rinse the sample.

hfacH residue remaining on the Si/SiO_2 surface after processing was readily removed by contacting with pure $scCO_2$.

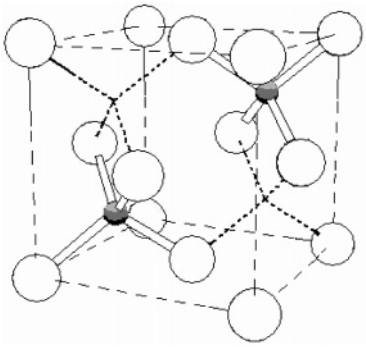

Figure 12. Cubic unit cell of $Cu(I)_4O_2$. Cu atoms (large open spheres) occupy face-centered cubic lattice positions and O atoms (small filled spheres) are in tetrahedral sites. Thick open lines indicate bonds between Cu and O. The interatomic distances to nearest neighbors are d(Cu−O) = 1.8 Å, d(O−O) = 3.7 Å, and d(Cu−Cu) = 3.0 Å.[45,46] Two of the remaining six empty tetrahedral sites are shown at the intersections of dark dashed lines. The relative atomic sizes and distances are not drawn to scale.

Discussion

Deposition from Cu-doped HF solutions produced $Cu(I)_2O$ islands with diameters of 10−90 nm primarily at the center of etching pits on a silicon surface. Close examination of the SEM image in Figure 2a shows faceting along the perimeter of some islands, which suggests crystalline structure. AFM imaging showed that the islands were approximately a factor of 2 times wider than they were high. The XPS and X-ray induced Auger spectra in Figure 3a and Figure 4a, respectively, show that the islands contained copper in a +1 oxidation state in the form $Cu(I)_2O$ produced in the Cu-doped aqueous HF solution during deposition or upon exposure to air afterward.[44] Since the photoelectron escape depth is on the order of the height, the bulk of the islands on the as-contaminated samples contained only $Cu(I)_2O$. The finite probe depth of approximately 20 nm, however, indicates that the thicker islands could also have contained Cu(0) metal. $Cu(I)_2O$ has the structure shown in Figure 12, where Cu atoms are at face-centered lattice sites and O atoms are at positions ($^1/_4$, $^1/_4$, $^1/_4$) and ($^3/_4$, $^3/_4$, $^3/_4$).[45,46] The hexagonal crystal structure observed for some islands in the SEM are consistent with the tetrahedral geometry of Cu atoms surrounding each O atom. $Cu(I)_2O$ is not a pure ionic crystal, however, with closed shell $3d^{10}$ Cu^+ ions as Zuo *et al.* have shown using quantitative convergent beam electron diffraction combined with X-ray diffraction.[46] Instead the Cu d states hybridize with unoccupied s and p states, accumulating charge in the empty Cu tetrahedral interstitial sites (two are identified by dark dashed lines in Figure 12) producing covalent Cu(I)−Cu(I) bonding.

Oxidation altered both the structure and composition of the copper islands, which played important roles in the two types of removal mechanisms observed using $scCO_2$. Oxidation of as-contaminated samples using aqueous 30% H_2O_2 changed the morphology of the Cu islands from flattened cylinders to flakes as shown by the top down and side view

(44) Belash, V. P.; Klimova, I. N.; Kormilets, V. I.; Trubitsin, V. Y. *Surf. Rev. Lett.* **1999**, *6* (3 & 4), 383.
(45) Ghijsen, J.; Tjeng, L. H.; van Elp, J.; Eskes, H.; Westerink, J.; Sawatzky, G. A.; Czyzyk, M. T. *Phys. Rev. B* **1988**, *38* (16), 11322.
(46) Zuo, J. M.; Kim, M.; O'Keeffe, M.; Spence, J. C. H. *Nature* **1999**, *40*, 49.

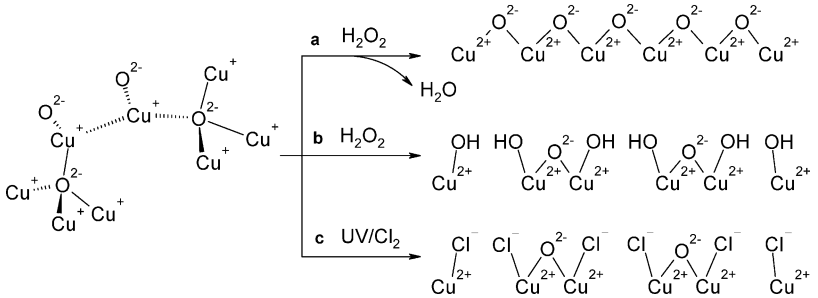

Figure 13. Oxidation of Cu(I) to Cu(II). Two Cu(I)O tetrahedra are shown linked by Cu−Cu bonding in an interstitial site. (a) Aqueous H_2O_2 oxidation of $Cu(I)_2O$ to Cu(II)O producing water. (b) Aqueous H_2O_2 hydroxylation of $Cu(I)_2O$ to $Cu(II)_2O(OH)_2$. (c) Gas-phase UV/Cl_2 chlorination of $Cu(I)_2O$ to $Cu(II)_2O(Cl)_2$.

SEM images in Figure 2b. Significantly more copper surface area was exposed in the flake structures, which is consistent with an increase in the surface roughness measured by AFM. The XPS spectra in Figure 5a and Figure 10a show that approximately half of the Cu(I) was oxidized to Cu(II) after the aqueous H_2O_2 step and the peak shift from Cu(I) to Cu(II) in the Auger spectrum in Figure 4b confirms this result. Two possible Cu(II) oxidation products using H_2O_2 are shown in Figure 13a and Figure 13b. In the first reaction, O atoms produced by decomposition of H_2O_2 insert at empty tetrahedral sites of $Cu(I)_2O$, where there is electron density due to Cu−Cu bonding,[46] forming Cu(II)O and water. In the second reaction, a hydroxylated copper oxide is produced by insertion of two hydroxyl radicals into unoccupied tetrahedral sites of $Cu(I)_2O$ forming $Cu(II)_2O(OH)_2$, which should be stable at the high pH of H_2O_2 solutions. Neither the XPS nor the Auger spectra can distinguish between the two products proposed for Cu(II) in the 30% H_2O_2 solutions. These overall reactions are consistent with the decomposition products of aqueous H_2O_2 on metal oxides.[47,48] Similar results were obtained using a subatmospheric gaseous UV chlorination process (Figure 9a) where the proposed reaction is insertion of Cl atoms into unoccupied interstitial sites of $Cu(I)_2O$ to form $Cu(II)_2O(Cl)_2$ (Figure 13c). Copper chlorides form polymeric chain structures in which planar $CuCl_4$ moieties share opposite edges, and Cu(II) oxides form oligomers.[49] These compounds are consistent with the insertion of oxidants into unoccupied tetrahedral sites, disrupting the Cu−Cu bonding and changing the morphology. Moreover, polymeric compounds may explain the low volatilities and the reason that standard halide or oxygen chemistries are not practical for plasma etching of copper.

Both the aqueous and gaseous oxidation processes produced a shell of Cu(II) surrounding a $Cu(I)_2O$ core. The XPS results (Figure 9a and Figure 10a) showed that approximately half of the Cu(I) initially present was converted to Cu(II). Since reaction must have occurred first at the exposed surfaces of islands and along grain boundaries of crystallites, the finite penetration depth of both conversion processes must have produced shells of Cu(II) surrounding cores of Cu(I) oxide. XPS, ion scattering spectroscopy (ISS),[50] photoacoustic spectroscopy,[51] and potentiometry[52] have shown that a bilayer film formed on Cu in alkaline $NaOH/NaClO_4$ solutions with an inner Cu_2O layer and an outer $CuO/Cu(OH)_2$ layer as a function of electrode potential. A corrosion study using XPS and SEM showed that a copper oxide film formed which limited dissolution of underlying Cu metal.[53] A gas-phase hfacH process at 203 °C and 10 Torr removed a Cu(II)O film formed in a previous furnace oxidation step but left a Cu(0) metal layer on Si,[16] which is also consistent with a shell and core model. The shells formed by aqueous H_2O_2 oxidation were thin flakes, as shown by SEM, composed of Cu(II). Self-limiting oxidation could be due to diffusion resistance of the Cu(II) oxide film to the oxidation precursors or due to the inhibition or recombination of the precursors on Cu(II) oxide surfaces. Cyclic voltammetry and UV−visible reflectance spectroscopy results were interpreted as showing that CuO surfaces inhibited the decomposition of H_2O_2.[54] Cl radicals produced in the gas phase have much higher diffusivities than the decomposition products of H_2O_2 in a liquid; consequently, the nearly identical amounts of Cu(I) and Cu(II) in the islands after oxidation using two different processes suggest that inhibition and recombination on the Cu(II) surfaces, rather than diffusion resistance, limited complete oxidation of the clusters.

A comparison of the results for fast and slow pressure release shows that there is a mechanical mechanism to selectively remove Cu(II)O from the surface. Based on the Auger and XPS spectra shown in Figure 4 and Figure 5, as well as the average removal percentage computed from several samples using XPS (Figure 6), the Cu(II)O shells were removed selectively to the $Cu(I)_2O$ cores by pure $scCO_2$ processes followed by rapid pressure release. A release rate of approximately 300 atm/min after the soak period achieved near complete removal, but a rate of 30 atm/min was insufficient to remove Cu(II)O (Table 3 and Figure 6, processes "a" and "b"). The pressure was released by opening the needle valve at the reactor outlet to an exhaust tube at

(47) Kitajima, N.; Fukuzumi, S.-I.; Ono, Y. *J. Phys. Chem.* **1978**, *82*, 1505.
(48) Wang, A. H.; Valentine, R. L. Hydrogen peroxide decomposition kinetics in the presence of iron oxides. In *Chemical Oxidation 3: Technologies for the Nineties*; Eckenfelder, W. W., Bowers, W. W., Roth, J. A., Eds.; Technomic Publishing AG: Basel, 1994; p 74.
(49) Greenwood, N. N.; Earnshaw, A. *Chemistry of the Elements*, 2nd ed.; Butterworth-Heinemann: Oxford, England, 1997.
(50) Strehblow, H.-H.; Titze, B. *Electrochim. Acta* **1980**, *25*, 839.
(51) Sander, U.; Strehblow, H.-H.; Dohrmann, J. K. *J. Phys. Chem.* **1981**, *85*, 447.
(52) Speckmann, H.-D.; Lohrengel, M. M.; Schultze, J. M.; Strehblow, H.-H. *Ber. Bunsen-Ges. Phys. Chem.* **1985**, *89*, 392.
(53) Feng, Y.; Siow, K.-S.; Teo, W.-K.; Tan, K.-L.; Hsieh, A.-K. *Corrosion* **1997**, *53* (5), 389.
(54) Vazquez, M. V.; de Sanchez, S. R.; Calvo, E. J.; Schiffrin, D. J. *J. Electroanal. Chem.* **1994**, *374*, 179.

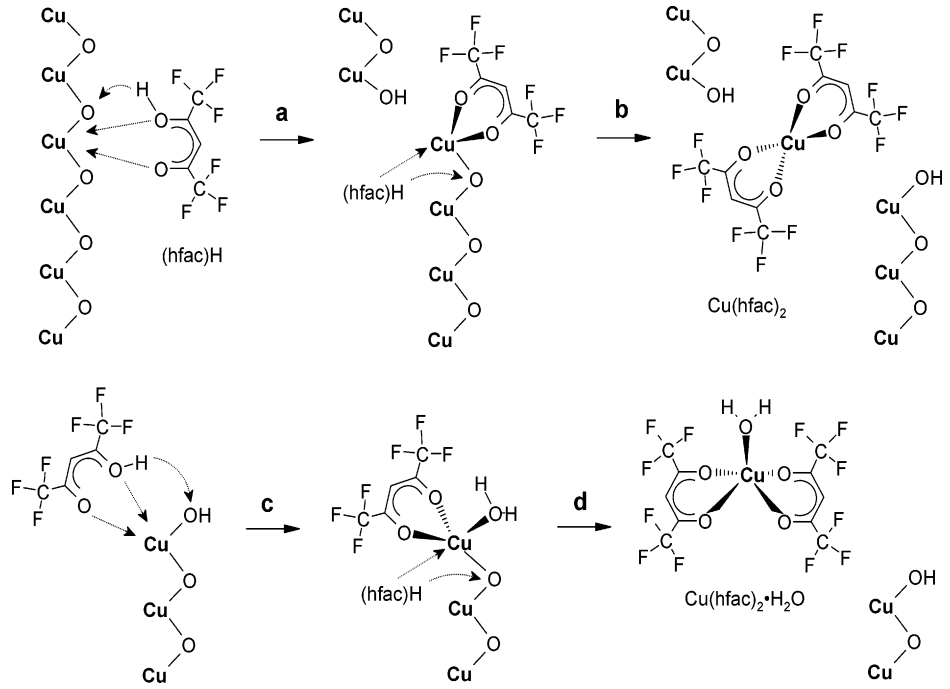

Figure 14. Schematic of proposed Cu(II)O removal mechanism. (a) Nucleophilic attack of hfacH on Cu(II) oxide (CuO) oligomer cleaving chain. (b) Attack of second hfacH molecule forming copper(bis-hexafluoroacetylacetonate), $Cu(hfac)_2$, which is soluble in $scCO_2$, and copper hydroxyoxide (Cu(OH)O) at ends of chain. (c) Reaction of hfacH with Cu(OH)O at oligomer end, producing Cu(II)hfac·H_2O surface complex. (d) Attack of hfacH on the surface complex producing copper(bis-hexafluoroacetylacetonate) monohydrate ($Cu(hfac)_2 \cdot H_2O$), leaving the end of the Cu(II)O chain hydroxylated.

atmospheric pressure. The drop in pressure created a flow across the sample surface toward the outlet of the reactor. Assuming an exponential decrease in the flow rate with time yields a fluid velocity of 3 cm/s across the sample surface based on the average flow rate of 3.3 mL/s and total release time of 60 s. A fluid element with a volume of 1 μm^3 and this velocity has a kinetic energy of 3×10^{-19} J or 160 kJ/mol, which is equivalent to a weak covalent bond. It is feasible that this energy was sufficient to break off the flake structures by momentum transfer as the reactor was emptied. A more likely mechanism for loss of Cu(II)O is by penetration of supercritical CO_2 into crevices in the flakes during the soak period followed by a rapid expansion of the CO_2 caused by a change in phase to a gas when the pressure was released. The sudden expansion could have delaminated the Cu(II)O, leaving $Cu(I)_2O$. This result shows that chemical specificity to remove Cu(II) relative to Cu(I) can be achieved using a mechanical force due to the different morphologies of the two oxides.

Complete removal of Cu with $scCO_2$ could only be obtained by partially oxidizing the Cu(I) to Cu(II) and using the metal chelator hexafluoroacetylacetone (hfacH). The necessity of the oxidation step is consistent with the literature where oxidants, such as Cl_2, O_2, O_3, and H_2O_2, have been shown to promote Cu etching in the gas phase using hfacH.[11−13,15,16] The experimental results using hfacH dissolved in $scCO_2$ support two different reaction mechanisms to remove copper depending on the oxidation state. Cu(II) reacted directly with two molecules of hfacH, producing $Cu(II)(hfac)_2$ and water or the monohydrate $Cu(hfac)_2 \cdot H_2O$. $Cu(I)_2O$, however, did not react directly with hfacH. Either hfacH or the reaction product of Cu(II) etching, namely, $Cu(II)(hfac)_2$, reacted with water, producing an oxidant. The resulting enol or monohydrate oxidized Cu(I) to Cu(II), allowing attack and removal by hfacH via the Cu(II) mechanism.

One possible removal mechanism for Cu(II) is transfer of the acidic proton on hfacH to an oxygen or chlorine atom bound to the Cu as shown in Figure 14a for Cu(II)O. Since this O atom is bonded to another Cu atom, the proton-transfer reaction frees the O end of a CuO moiety from the polymer-like network, forming a hydroxyl group. Nucleophilic attack on Cu(II) by the two O atoms on the conjugated partial ring of the hfac anion completes the first step in the reaction. The remaining bond holding the Cu atom is broken by reaction with another hfacH molecule, which transfers a proton to O and terminates the other chain with a hydroxyl group (Figure 14b). The product is copper(bis-hexafluoroacetylacetonate), $Cu(hfac)_2$. Two hfacH molecules are needed to completely free a Cu atom from the CuO lattice to satisfy the bonding requirements of a Cu atom, which usually forms square or square pyramidal structures with O.[49] The Cu complex $Cu(hfac)_2$ is soluble in $scCO_2$ (3.54×10^{-3} mole fraction at 40 °C and 175 atm).[55] The hydroxylated ends of the CuO chain undergo similar reactions, producing $Cu(hfac)_2$ and water or $Cu(hfac)_2 \cdot H_2O$ (Figure 14c and 14d). The mixed Cl and O containing Cu(II) would also produce HCl due to proton transfer from hfacH to Cl. The Cu-bearing products are used to deposit copper,[5,32,33] but without a reducing agent no net deposition was expected and none was observed below 60 °C and 225 atm in the $scCO_2$ etching experiments.

Cu(II)O has been etched using both gas and supercritical CO_2 phases. George *et al.* used a two-step all gas-phase processing sequence to remove Cu using hfacH.[16] A furnace oxidation of a thin layer of Cu on a Si wafer at 350 °C in air for 4 h formed Cu(II)O in the first step, which was

(55) Erkey, C. *J. Supercrit. Fluids* **2000**, *17*, 259.

Table 4. Molar Ratios of Oxygen and Water Vapor in $scCO_2$ Reactor Air to Copper and HfacH during Processing Based on 1 × 10^{16} Cu atoms/cm^2

O_2/Cu	45 000
hfacH/Cu	9000
water vapor/Cu	2000
O_2/hfacH	5
water vapor/hfacH	0.3

verified by combining the XPS Cu $2p_{3/2}$ and Cu($L_3M_{4,5}M_{4,5}$) Auger transitions into an Auger parameter. After processing in a gas phase consisting of 25% hfacH in N_2 at 203 °C and 10 Torr for 5 min in the second step, all of the Cu(II) oxide was removed but Cu(0) metal was left on the surface. The nominally 170 nm Cu(II) oxide film grown by George *et al.* was continuous compared to the clusters used in this study. The aqueous H_2O_2 and gas-phase UV−Cl_2 processes used here consequently may have oxidized a larger percentage of the Cu(I) to Cu(II) because of the higher surface area exposed. Steger and Masel showed that a continuous gas flow of 50 Torr hfacH and 200 Torr O_2 at 350 °C etched copper coupons at 1.65 μm/min.[13] Decreasing the temperature to 300 °C and the pressure below 200 Torr reduced the etching rate by an order of magnitude. They attributed the decrease to the mixture of Cu(I) and Cu(II) oxides produced below 325 °C, in contrast to the Cu(II)O formed at 375 °C. Bessel *et al.* also combined the oxidant and etchant into a single-step process to etch copper coupons using $scCO_2$.[36] Based on the Cu $2p_{3/2}$ XPS peak, the copper surfaces were covered with $Cu(I)_2O$ initially and a mixture of $Cu(I)_2O$ and Cu(II)O after processing for 18 h in a mixture of ethyl peroxydicarbonate (1 equiv) to hfacH (2 equiv) at 40 °C and 214 bar and rinsing with hexanes. Weight loss measurements produced a nominal etching rate of 158 layers of Cu/min or approximately 0.05 μm/min. AFM measurements showed that the surface was heterogeneous after processing with the organic oxidant and hfacH mixture in $scCO_2$, and the roughness increased by approximately a factor of 5. The surface heterogeneity observed could be a result of the difference in morphology between $Cu(I)_2O$ and Cu(II)O as shown here. The surface concentrations of the two oxides in a single-step process will be a function of the oxidant and hfacH concentrations in the fluid phase, interactions between the oxidant and hfacH, and the relative reaction rates for Cu(I) oxidation to Cu(II) and Cu(II) removal, since the oxidant is always present.

Cu(I) was etched by the series oxidation and removal processes used in this study, but only when both Cu(II) and hfacH were present. A mixture of hfacH and $scCO_2$ did not remove Cu(I) from as-contaminated samples (Figure 8), unless samples were given a prior exposure to an oxidant (Figure 9 and Figure 10). Since Cu(I) had to be oxidized in order to be removed by hfacH, the oxidant must have been present in the reactor at the start of the experiment or produced by the reaction that removed Cu(II). The reactor was not purged prior to a $scCO_2$ process so a volume of air at ambient conditions was present initially before the reactor was filled with liquid CO_2 and included in the reaction mixture for every experiment. An estimate of the O_2 and water vapor in this air volume shows that the molar ratio of these oxidants to Cu atoms was high (Table 4). Barnartt *et al.* found that Cu metal coupons reacted with neat liquid acetylacetone (nonfluorinated) at 30 °C when O_2 was bubbled through the solution forming copper diacetylacetonate, $Cu(acac)_2$, but not when N_2 was used.[56] The oxidation of Cu(I) by O_2 or *both* O_2 and water is thermodynamically favorable at 50 °C only when there is a supply of electrons or a Lewis base in the mixture (Table 5). However, direct oxidation of Cu(I) by O_2 and water vapor during $scCO_2$ processing was insignificant since every experiment included the same quantity of air. For the same reason the major contaminants in the CO_2, which were ammonia, carbon monoxide, hydrogen sulfide, nitric oxide, nitrogen dioxide, hydrocarbons, and sulfur dioxide, did not participate in the Cu removal process.

Table 5. Gibbs Free Energy Changes for Cu(I) Oxidation Reactions Involving Oxygen, Water, Hydrogen Peroxide, and Hydrochloric Acid[61]

reaction	$\Delta G°$ at 50 °C (kJ/mol)
$Cu(I)(s) + e^- + (1/2)O_2(g) = Cu(II)O(s)$	−174
$Cu(I)(aq) + e^- + H_2O(l) = Cu(II)O(s) + H_2(g)$	+53
$Cu(I)(aq) + e^- + H_2O(l) + (1/2)O_2(g) = Cu^{II}(OH)_2(s)$	−167
$Cu(I)(aq) + e^- + H_2O_2(l) = Cu(II)O(s) + H_2O(l)$	−292
$Cu(I)(s) + e^- + 2HCl(aq) = Cu(II)Cl_2(s) + H_2(g)$	+38

The water or HCl produced by the reaction of hfacH with Cu(II)O and $Cu(II)Cl_2$, respectively, could have provided the oxidant needed to remove the Cu(I) cores, once the Cu(II)O or $Cu(II)Cl_2$ shells were removed. Sievers *et al.* showed using gas chromatography and visual observations that reaction of scandium metal with some β-diketones including hfacH at 170 °C was catalyzed by water.[57] They proposed that hfacH reacts with two water molecules to produce 1,1,1,5,5,5-hexafluoro-2,2,4,4-tetrahydroxypentane. The reaction of Cu with hfacH and water was not reported in that study probably because no dissolution was found for Cu using another β-diketone, heptafluorodimethyloctanedione, in a set of screening experiments. Both the tetrahydroxypentane and the intermediate trihydroxy species are polar, however, since the electron-withdrawing trifluoromethyl moieties increase the acidity of the O−H groups. These species consequently will have much lower solubilities in nonpolar CO_2 than hfacH. Another plausible oxidant is $Cu(hfac)_2{\cdot}H_2O$, which is a product of Cu(II) removal as shown in Figure 14. Moreover, $Cu(hfac)_2$ readily converts to the monohydrate $Cu(hfac)_2{\cdot}H_2O$ when exposed to water.[58] Oxidation of $Cu(I)_2O$ by the monohydrate could occur as shown in Figure 15, where two $Cu(I)_4O^{2-}$ tetrahedra are shown linked by a Cu(I)−Cu(I) bond.[46] Cleavage of a Cu(I)−O bond occurs by the concerted attack of an OH radical on Cu(I) producing Cu(II)−OH and donation of H to the O yielding an O−H group (reaction a). The Cu−Cu bond is also broken by this process, making the other Cu(I) atom more susceptible to oxidation by $Cu(hfac)_2{\cdot}H_2O$ in reaction b. The Cu(II)−OH products of these reactions are attacked by hfacH as shown by reaction c in Figure 14 yielding $Cu(hfac)_2{\cdot}H_2O$. A similar set of

(56) Barnartt, S.; Charles, R. G.; Littau, L. W. *J. Phys. Chem.* **1958**, *62*, 763.
(57) Sievers, R. E.; Connolly, J. W.; Ross, W. D. *J. Gas Chromatogr.* **1967**, *5*, 241.
(58) Funck, L. L.; Ortolano, T. R. *Inorg. Chem.* **1968**, *7* (3), 567.

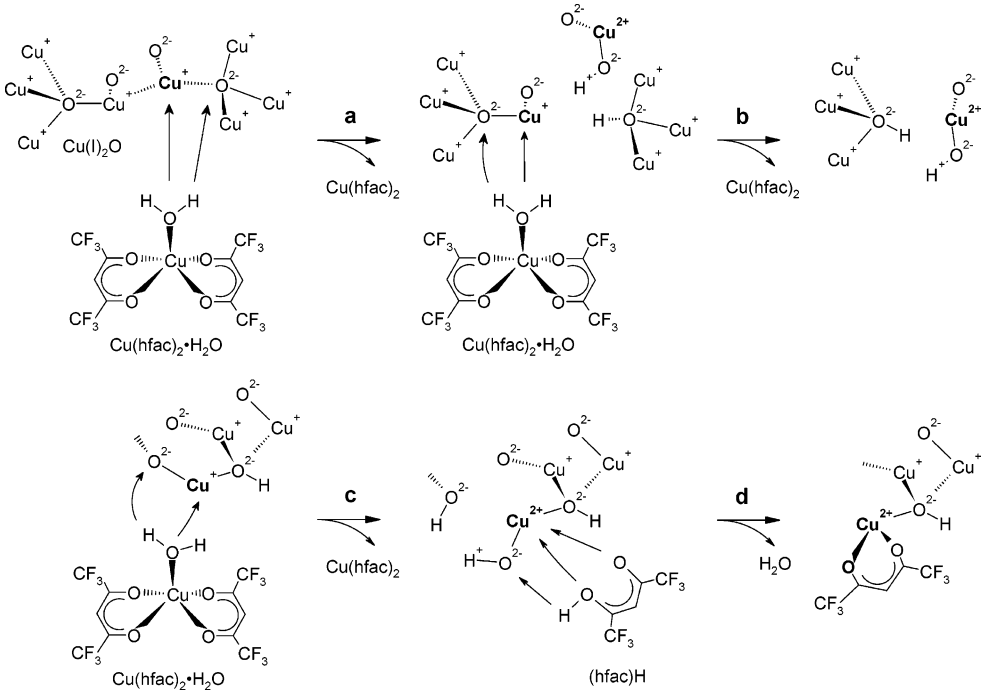

Figure 15. Schematic of proposed $Cu(I)_2O$ removal mechanism. (a) Oxidation of Cu(I)−O bond by the monohydrate Cu(II)hfac·H_2O, breaking the Cu−Cu bond and producing Cu(II)−OH and Cu_3O−H. (b) Oxidation of the $Cu(I)O_2$ moiety by Cu(II)hfac·H_2O, yielding Cu(II)−OH and Cu_3O−H. (c) Oxidation of $Cu(I)_3O$−H by Cu(II)hfac·H_2O to $Cu(II)(OH)_2$ and O−H. (d) Etching of $Cu(II)(OH)_2$ by hfacH.

reactions occurs for the Cu(I)−OH produced, which is first oxidized by the monohydrate to Cu(II)−OH and then etched with hfacH to remove Cu (reactions c and d in Figure 15). The $Cu(hfac)_2$, $Cu(hfac)_2$·H_2O, and water produced act catalytically in the removal of Cu(I). The HCl produced by the reaction of hfacH and $Cu(II)Cl_2$ participates in an analogous reaction sequence.

The proposed mechanism for Cu(I) etching is supported by the hfacH experiment in the cleanroom where Cu(I) was removed without Cu(II)O present (Figure 3). In contrast to the $scCO_2$ experiments where the water concentration was low (Table 4), water vapor comprises approximately 1% of cleanroom air. In addition, pure liquid hfacH, which is hygroscopic,[58] was placed directly on the sample surface. The concentrations of both hfacH and water vapor in the cleanroom ambient experiment were consequently several orders of magnitude higher than those in the $scCO_2$ processes. Oxygen was present at a much higher concentration than water vapor in both the air in the reactor and in the cleanroom and Barnartt *et al.* showed that O_2 is necessary for Cu(0) metal to react with liquid acetylacetone.[56] However, the O_2 concentration in the $scCO_2$ experiments was approximately 700 ppm or 5 times the hfacH concentration on a molar basis, which indicates that O_2 acts in combination with water, if it participates at all in the Cu(I) etching reaction.

Most of the previous work to etch Cu using hfacH was done with continuous gas flow processes. This work extends those results and shows that batch processing in a supercritical fluid at low temperatures is possible. Instead of forming a volatile product as in a gas-phase etching reaction, the product must be soluble in a $scCO_2$ fluid cleaning process to be removed from the surface. The hexafluoro variant of acetylacetone was chosen for this study because the solubility in $scCO_2$ increases by an order of magnitude for each methyl side group that is completely fluorinated.[55] There are disposal issues associated with F bearing compounds, however, since F persists in the environment. Using a mole fraction value of 3.54×10^{-3} for the solubility of $Cu(hfac)_2$ in $scCO_2$[55] yields a $scCO_2$ volume of only 3×10^{-5} mL to solvate one layer of Cu atoms per cm^2 surface area. Scaling to a 300 mm (12 in.) wafer size, the capacity of $scCO_2$ for $Cu(hfac)_2$ indicates that less than 100 mL/min of $scCO_2$ is needed to support an etching rate of 1 μm/min. This number must be used with caution, however, since it is valid only for an equilibrium process and solubilities in $scCO_2$ often change dramatically over a relatively narrow density range. Laintz *et al.*[59] show that the extraction of Cu(II) from a silica surface using a lithium bis(trifluoroethyl)dithiocarbamate (LiFDDC) complexant doubled when the $scCO_2$ density was increased from 0.29 to 0.37 g/cm^3. This estimate and the processing times on the order of minutes to achieve complete removal suggest that $scCO_2$ processing is industrially viable for cleaning Cu from surfaces and perhaps for etching Cu, which deserves further study.

Acknowledgment. The work was supported by the NSF/SRC Engineering Research Center for Environmentally Benign Semiconductor Manufacturing (NSF EEC-9528813 and SRC 2001-MC-425).

CM048111A

(59) Laintz, K. E.; Wai, C. M.; Yonker, C. R.; Smith, R. D. *Anal. Chem.* **1992**, *64*, 2875.
(60) Moulder, J. F.; Stickle, W. F.; Sobol, P. E.; Bomben, K. D. *Handbook of X-ray Photoelectron Spectroscopy*; Perkin-Elmer Co.: Minnesota, 1995.
(61) Lide, D. R. *Handbook of Chemistry and Physics*, 81st ed.; CRC Press: Boca Raton, FL, 2000.